Quantum delocalization and correlation effects in one-dimensional chains of adsorbed hydrogen atoms

Benjamin Berberich* and Axel Groß
Institut für Theoretische Chemie, Universität Ulm, D-89069 Ulm, Germany
(Dated: October 13, 2010)

Quantum delocalization and correlation effects in one-dimensional chains of bosons are treated using a Bose-Hubbard Hamiltonian including on-site and nearest-neighbor repulsion terms. The parameters were chosen in such a way that the calculations are appropriate for hydrogen atoms adsorbed in the troughs of fcc(110) surfaces. Employing direct diagonalization of the Hamilton matrix for small periodic systems, we find that the hydrogen atoms are always delocalized except for half-filling corresponding to a coverage of $\rho = 1/2$ where an ordered structure results for small tunnel parameters and sufficiently large nearest-neighbor repulsion, in accordance with experimental findings. For this coverage, a phase diagram as a function of the tunnel parameter and the nearest-neighbor repulsion is determined. Only if the translational invariance of the chain is perturbed, ordered structures for other coverages can be created. Larger systems are studied using the density matrix renormalization group (DMRG) algorithm. Using the finite length version of the DMRG algorithm, we find ordered states also for coverages of $\rho = 1/3$ and $1/4$ which are obviously a consequence of the perturbation caused by the termination of the finite chains.

PACS numbers: 68.43.Fg, 68.35.Rh, 67.63.Gh, 67.90.+z

I. INTRODUCTION

There is currently a strong interest in tailored quantum matter confined in reduced dimensions or in periodic lattices[1]. They allow to study fundamental phenomena such as decoherence and quantum phase transitions in strongly correlated systems which are relevant for, e.g., quantum computing. Typically cold atoms trapped in optical lattices have been employed to prepare such systems[2]. However, nature provides a template for the trapping of quantum particles in a periodic lattice that can be prepared with a high degree of perfection, namely low-index single-crystal metal surfaces[3]. Via adsorption, these surfaces can host light particles such as hydrogen that exhibit quantum phenomena such as delocalization and correlation[4,5].

The diffusion of hydrogen atoms on such metal surfaces is hindered by relatively small barriers[6,7]. It has been realized already quite long ago that because of these small barriers hydrogen atoms can become delocalized at low temperatures forming single-particle Bloch waves[4,5,8–11]. This leads to protonic vibrational bands[12], analogous to the electron bands formed by the conduction electrons of metals. These vibronic states can be detected by measuring the vibrational spectra of adsorbed hydrogen atoms[13]. From the band width of the vibrational bands the degree of delocalization of the hydrogen atoms can be deduced[5]. In passing, we note that there is still a discussion going on whether adsorbed hydrogen atoms should be regarded as bosons or as fermions[5]. Furthermore, quantum effects in the hydrogen adsorption dynamics are also still debated[14–18].

Experimentally, it has been observed that the band width of excited hydrogen-derived vibronic bands on the (110) surfaces of Cu[13] and Pd[19] decreases for higher hydrogen coverages. Theoretically, the system was modeled by a simple one-dimensional Bose-Hubbard-like Hamiltonian for one vibrationally excited hydrogen atom subject to a repulsive interaction with fixed ground-state hydrogen atoms[13]. The restriction to a one-dimensional model was based on the assumption that the hydrogen atoms only move along the $[1\bar{1}0]$ troughs of the (110) surface and do not interact with hydrogen located in other troughs. The repulsion between the hydrogen atoms leads to an effective localization of the vibrationally excited hydrogen atom which reduces the band width of the vibronic bands, as reproduced by the simple Bose-Hubbard-like model[13,19]. Single-particle delocalization effects of adsorbed hydrogen have also been observed on a number of other single crystal surfaces (see Ref. 5 and references therein).

As a function of the hydrogen coverage, not only one-particle quantum effects can be observed, but also many-body quantum effects such as quantum phase transitions, i.e., phase transitions that are not induced by temperature but by the change of a physical parameter at zero temperature. For example, in the H/NiAl(110) system, at low coverages a 1×1 hydrogen structure was observed[20] that was interpreted as being due to delocalized itinerant hydrogen. At coverages between 0.4 and 0.6, a $c(2 \times 2)$ hydrogen structure is observed, however, with such a shallow corrugation amplitude that it was taken as evidence for the delocalization of hydrogen in this ordered phase[20,21].

It is important to realize that the Bose-Hubbard studies of hydrogen atoms on fcc(110) surfaces performed so far[13,19] just treated single-particle quantum effects. Thus collective quantum phenomena of adsorbed hydrogen atoms were not addressed. At low temperatures, the quantum nature of the hydrogen atoms should be relevant for the adsorption structures that evolve. To describe this properly, a real many-particle picture in the

language of second quantization is needed. However, a direct solution of the appropriate Hamiltonian is computationally very costly because of the rapidly growing Hilbert space of the system as a function of the system size. This makes it necessary to use the theory of quantum phase transitions and quantum mechanical renormalization groups.

It is true, that there have already been several studies addressing bosonic particles in one-dimensional chains using Bose-Hubbard models in second quantization together with renormalization group algorithms[22,23] or Monte Carlo methods[24]. Hence it is well-known that in the presence of on-site interactions only, so-called Mott insulators are found at integer densities surrounded by superfluid phases[25,26], whereas the introduction of nearest-neighbor interaction leads to charge-density waves at half-integer densities[23]. However, these theoretical studies were not necessarily driven to simulate a particular physical system but rather to understand the generic behavior of one-dimensional bosonic systems. Here we have a well-defined physical system in mind, namely the adsorption of hydrogen atoms in a periodic one-dimensional structure provided by a metal substrate. Hence the physical parameters entering the corresponding Bose-Hubbard Hamiltonian, in particular the on-site and the nearest-neighbor repulsion, are no longer free parameters. Rather, they should reflect the properties of a particular system. They can be derived either empirically from experiments or from first-principles calculations[27] which are predominantly based on density functional theory (DFT). Since typically every adsorption site can only be occupied by one hydrogen atom which is reflected by a large on-site repulsion term, the filling or rather the coverage can not exceed one. To the best of our knowledge, this particular parameter regime with a dominant on-site repulsion has not be scrutinized in one-dimensional Bose-Hubbard models yet.

Thus one aim of this work is it to close the gap between studies related to quantum delocalization phenomena on surfaces and work addressing quantum phase transitions in a more generic sense. To do so, in the following we will first recall some basics about the Bose-Hubbard model and its relevance to surface problems. In the second step we study ideal small one-dimensional systems with periodic boundary conditions using a full diagonalization scheme. We will also consider the influence of a small perturbation on the periodicity of the solution. Finally we will focus on large finite systems employing the density matric renormalization group algorithm[28–30].

II. THE BOSE-HUBBARD MODEL

The Hubbard model was originally introduced to study the magnetic properties of electrons in transition metals[31]. Since then, the Hubbard model has been applied to a wide range of fermionic systems, in particular with respect to the theoretical description of high-temperature superconductors[32]. Bosonic Bose-Hubbard Hamiltonians have mainly been applied to neutral atomic gases trapped in optical lattices[33]. As already mentioned, Astaldi *et al.* were the first to use the Bose-Hubbard Hamiltonian for a surface science problem[13], namely for the description of hydrogen atoms adsorbed in the one-dimensional troughs along the $[1\bar{1}0]$ direction of a fcc(110) surface. In the general formulation in second quantization, the Bose-Hubbard Hamiltonian reads, including on-site (OS) and nearest-neighbor (NN) repulsion terms,

$$\begin{aligned} H &= \underbrace{-T\sum_{i=1}^{L}(a_{i-1}^{+}a_i + a_i a_{i+1}^{+})}_{\text{hopping term}} + \underbrace{\frac{1}{2}U\sum_{i=1}^{L} n_i(n_i-1)}_{\text{OS-repulsion}} \\ &+ \underbrace{V\sum_{i=1}^{L} n_i n_{i+1}}_{\text{NN-repulsion}} \quad . \end{aligned} \tag{1}$$

In our particular application, the single indices i stand for the adsorption sites along the one-dimensional troughs. In the following we consider L adsorption sites within the troughs and refer to the troughs as "chains". To treat extended system, we apply periodic boundary conditions so that effectively we obtain "rings" with the last site being the direct neighbor of the first site.

In eq. (1), a_i^{+} and a_i stand for the bosonic creation and annihilation operator, respectively, at site i and $n_i = a_i^{+}a_i$ denotes the occupation number operator. The tunneling or hopping term describes the hopping of a particle from one site to a direct neighbor site with the parameter T being related to the overlap between the localized wave functions at the single sites. The OS-repulsion term then introduces a repulsion U for particles occupying the same adsorption site. Finally, the NN-interaction V reflects the repulsion between particles in neighboring sites. The operator itself carries no information about how many hydrogen atoms N are adsorbed on the L sites or, in the language of our picture, how may particles are in the chain. The information of the particle density $\rho = N/L$ is contained in the basis of the corresponding Hilbert space. Since we consider the adsorbed H-atoms to be bosons, this space $\mathcal{H}$ is given by

$$\mathcal{H} = span\{\ |k_1, ..., k_L\rangle\ : k_i = 0, ..., N\ ; \sum_{i=1}^{L} k_i = N\}, \tag{2}$$

where k_i is the occupation number of site i. The dimension of such a space is given by

$$\begin{aligned} d &= dim\ \mathcal{H} = \binom{L+N-1}{N} \\ &= \frac{(L+N-1)!(L-1)!}{N!}, \end{aligned} \tag{3}$$

Equation (3) shows, that the dimension of the considered bosonic systems grows drastically with the size parameters L and N. For example, the routines embedded in

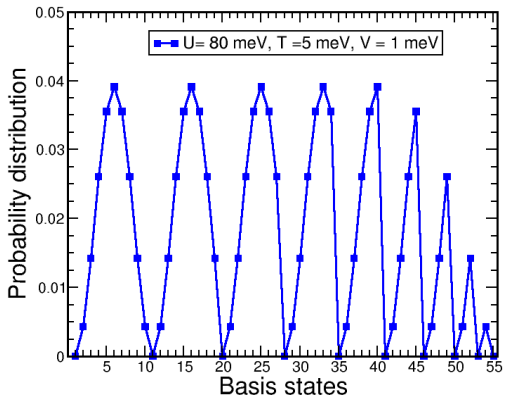

FIG. 1: Probability distribution of finding one of the 55 basis states in the expansion of the ground state. See the text for an explanation of the ordering of the basis states.

the full diagonalization program used in section V are only able to handle fully covered chains ($\rho = 1$) within a reasonable computational time for chain lengths $L \leq 8$.

III. SIMPLE PROBABILITY SPECTRA

In order to understand the resulting distribution of the hydrogen atoms along the chain, we will first discuss the energy eigenvalue spectrum. As an example, we consider a system with $N = 2$ particles in a chain of $L = 10$ sites with periodic boundary conditions corresponding to a filling or coverage of $\rho = 1/5$ using the parameters suggested by Astaldi *et al.*[13]: $U = 80$ meV, $V = 1$ meV, $T = 5$ meV. Note that these parameters were chosen in order to represent an adsorbed hydrogen atom in a higher vibrational state, in which the atomic wavefunction is spread out to a larger extent than in the vibrational ground state. Therefore the on-site repulsion U is much smaller and the overlap parameter T is much larger compared to the parameters chosen to represent vibrational ground state systems considered in section V.

For the considered system with $N = 2$ and $L = 10$ the Hilbert space has the dimension $d = 55$ according to eq. (3). Diagonalizing the Hamilton matrix leads to 18 distinct energy eigenvalues. They can be divided into four groups related to the energy parameters of the system:

$$\begin{aligned} &\text{I}) && \pm 4T && \approx -19.1;\ 19.0 \text{ meV} \\ &\text{II}) && \pm 3T && \approx -15.5;\ -15.4;\ 15.2;\ 15.4 \text{ meV} \\ &\text{III}) && \pm 2T && \approx -12.1;\ -9.6;\ -9.5;\ 9.3;\ 9.5;\ 11.3 \text{ meV} \\ &\text{IV}) && U && \approx 80.0;\ 80.2;\ 80.9;\ 81.6;\ 82.3;\ 82.5 \text{ meV} \end{aligned} \quad (4)$$

We will now use the occupation number representation outlined in eq. (2) to discuss the energy spectrum extending an interpretation made in Ref. [13]. The basis states are ordered as follows. State 1 is given by both particles occupying the first site,

$$\mathbf{e}_1 \equiv |2000000000\rangle \ . \quad (5)$$

The next states are created by keeping one particle at site 1 and moving the other particle along the chain. Then the first particle is set to the second site and the second particle is again moved along the chain. Note that states that correspond to an exchange of the particles are not considered twice because of the indistinguishability of the particles. There are in each case ten laterally equivalent states in which the particles are zero to four lattice sites apart from each other and five equivalent states in which the particles have the maximum distance of five sites.

In the analysis of the energy spectrum, we will consider the probability expansion of a representative state of each group. For group I, we pick the ground-state with energy $E_0 = -19.1$ meV. Its expansion in terms of the 55 basis states is given in Fig. 1. Maximum occupation is found for states such as

$$\mathbf{e}_6 \equiv |1000010000\rangle \quad (6)$$

and the five translational equivalent situations. These correspond to situations in which the particles have the largest possible distance from each other, namely five lattice sites. Hence the atomic positions are correlated over a longer distance than the actual range of the NN-repulsion.

Inspecting the state (6), it is obvious that both particles can jump to the "right" and to the "left" without getting in contact with each other. So in the situations (6) the system has 4 unconditional degrees of freedom. The same is true for states with the particles being 4 and 6 sites apart from each other which also contribute to the ground state shown in Fig. 1. This explains the energy value of $E_I \approx \pm 4T$, but this also means that the correlation length is less than four lattice sites.

Analogous explanations are also applicable to the other three energy groups listed in (4). Analyzing the first excited state as a representative of group II reveals that the highest occupation occurs for states such as

$$\mathbf{e}_4 \equiv |1001000000\rangle \quad (7)$$

In states such as (7), just one particle can jump without being influenced by the position of the second particle. The second particle can directly be affected by the movement of the first particle. To be specific, just assume that one particle described in (7) jumps towards the other. In this case, the other particle can only jump into one direction without any energy cost since a jump into the other direction costs the NN-repulsion V. Thus we can identify 3 unconditional degrees of freedom reflected in the total energy $E_{II} \approx \pm 3T$.

Looking at the remaining 2 energy groups one can observe that the members of group III are dominated by

basis states such as

$$\mathbf{e}_9 \equiv |1000000010\rangle \tag{8}$$

in which the particles have just 2 unconditional degrees of freedom; therefore an total energy of $E_{III} \approx \pm 2T$ results. Finally, group IV states consists mainly of basis states given by Eq. (5) corresponding to a situation in which two hydrogen atoms are located at the same adsorption site associated with the high energy cost U of the OS-repulsion.

This discussion shows that in spite of the fact that the Hamiltonian (1) only includes on-site and nearest-neighbor repulsion, the position of the particles is correlated over much larger distances.

IV. PHASES OF THE BOSE-HUBBARD MODEL

In contrast to the surface science studies performed so far[13,19], we do not want to restrict ourselves to one-particle quantum effects but rather address many-particle quantum effects, in particular quantum phase transitions as a function of the coverage. To denote the phases and make contact to previous work, we will use the terminology commonly used to characterize quantum many-particle states although they do not really make sense for the systems considered by us, hydrogen atoms adsorbed on metal surfaces in linear troughs. For the Bose-Hubbard model with NN-interaction, three possible phases can be expected[22]. For coverages lower than $\rho = 1$ there is the opportunity to find either a *Suprafluid Phase* (SF phase) or a *Charge Density Wave Phase* (CDW). If we consider coverages ρ or filling factors corresponding to positive integers, we have the additional possibility of finding a *Mott-Insulator Phase* (MI phase).

In the context of the delocalization problem of bosons the MI and CDW phases are just interpreted as localized phases and the SF phase stands for a delocalized state. To distinguish between them we introduce the *local density* (9)

$$\rho_i \equiv \langle \hat{n}_i \rangle \tag{9}$$

Qualitatively, the following trends in the quantum delocalization as a function of the parameters entering the model can be expected. Increasing the kinetic energy T increases the mobility and thus the delocalization of the phases leading eventually to a SF-Phase. A higher NN-repulsion V, on the other hand, keeps the particles apart from each other favoring a CDW. Likewise, a higher coverage ρ increases the atom-atom interaction and hence restricts the mobility. Consequently, enlarging ρ should also lead to localization effects in a similar manner as described in[13]. The possible phases are characterized in Table (I).

V. PERIODIC SYSTEMS

In a first step, we determine the quantum phases as a function of the tunneling parameter T, the NN-repulsion V and the hydrogen coverage in periodic chains with a relatively short length L of the periodic region so that the solutions of the Bose-Hubbard Hamiltonian (1) can still be obtained by direct diagonalization. The parameters entering the Hamiltonian are chosen in such a way that they reflect properties of hydrogen atoms adsorbed on single-crystal surfaces. For any particular hydrogen/metal system, these parameters are given and can be derived from first-principles calculations. However, there is a wide range of possible surface structures and compositions, all with their own characteristic hydrogen-metal interaction. Therefore we have decided to consider a certain realistic range of parameters found in total energy calculations.

The nearest-neighbor repulsion V can be derived from first-principles studies based on density functional theory (DFT) in which the adsorption energy of hydrogen on metal surfaces as a function of coverage was determined[34–39]. For example, for H/Pd(210) a value of $V = 25\,\text{meV}$ can be derived[37]. Hence, a range $10\ \text{meV} \leq V \leq 200\ \text{meV}$ seems to be reasonable.

The overlap parameter T can be related to the width W of hydrogen vibronic bands. Here we will assume $W = 8T$ where W is the width of the band. This is only strictly valid for the case of a two-dimensional square lattice in the tight-binding approximation with only next-nearest neighbor interaction, however, this should be sufficient as an estimate.

The width W has been derived for several hydrogen adsorption system based on potential energy surface calculated using DFT. On (100) surfaces, the corresponding tunnel parameters are extremely small. Tunnel amplitudes of $T = 2 \cdot 10^{-7}\,\text{meV}$ (H/Ni(100)[40]) and $T = 5 \cdot 10^{-11}\,\text{meV}$ (H/Cu(100)[41]) have thus been obtained. At the (100) surface, the hydrogen atoms are adsorbed on four-fold hollow sites which are relatively far away from each other. On the close-packed (111) surfaces, the first-principles derived tunnel parameter are much larger, namely $T = 0.5\,\text{meV}$ for H/Ni(111) [8] and H/Rh(111) [42], $T < 0.01\,\text{meV}$ for H/Pt(111) at fcc sites and $T = 0.2\,\text{meV}$ for H/Pt(111) at hcp sites[12]. Since we are considering one-dimensional rows of adsorption sites along some close-packed directions, we have assumed the parameter T to be in the range $0.01\ \text{meV} \leq T \leq 0.1\ \text{meV}$.

Usually every adsorption site on metal surfaces hosts only one hydrogen atom. Additional hydrogen either does not stick or enters subsurface absorption sites[4,43,44]. These observations should be reflected by a large OS-repulsion term U and coverages with $\rho \leq 1$. In order to estimate a typical value for U, we performed periodic DFT calculations[45] for two hydrogen atoms on Pd(100) modeled by a five-layer slab within a 4×4 surface unit cell using the generalized gradient approximation[46] to describe the exchange-correlation effects. Two hydrogen

phases	SF	CDW	MI
Local Density	$\rho_i \in \mathbb{Q}$ and $\rho_i = \frac{N}{L}$	$\rho_i \in \mathbb{R}$ and $\rho_i \neq const.$	$\rho_i \in \mathbb{N}$ and $\rho_i = \frac{N}{L}$
Ground-state $L = \infty$	degenerate	degenerate	not degenerate
Ground-state $L < \infty$	not degenerate	degenerate	not degenerate
Interpretation	delocalized	localized	localized

TABLE I: Characterization of the three possible quantum phases of a one-dimensional bosonic system described by a Bose-Hubbard model for infinite and finite chain length L.

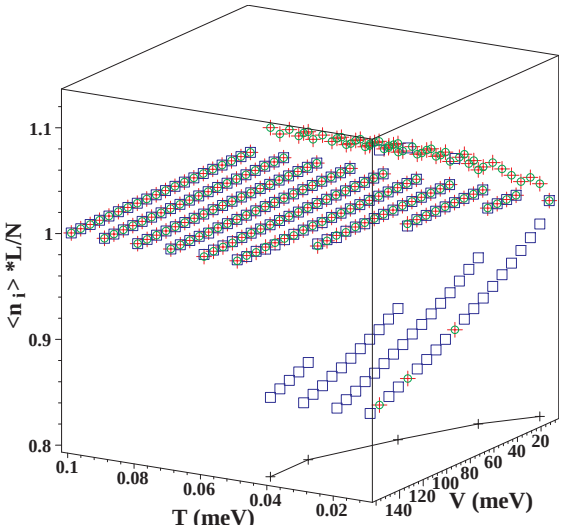

FIG. 2: Renormalized local densities $\rho_1 \equiv$ crosses, $\rho_2 \equiv$ squares and $\rho_3 \equiv$ circles over T and V for $L = 8$, $N = 4$ and $U = 1000$ meV. The black line is the projection line of the phase boundary into the V-T plane.

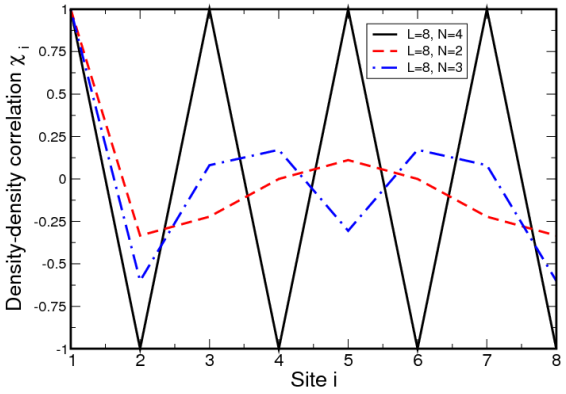

FIG. 3: Normalized density-density correlation function χ_i (eq. (11)) for $L = 8$ and $N = 2, 3, 4$. The particular parameters are $U = 1000$ meV, $T = 0.02$ meV and $V = 70$ meV.

atoms ontop of each other at the fourfold-hollow site are 880 meV more costly than at their maximum distance within the 4×4 surface unit cell. Hence we have selected a value of $U = 1000\,\text{meV}$ to represent this large on-site repulsion. Note that the chosen parameter range lead to ratios of $T/V \leq 10^{-2}$ and $T/U \leq 10^{-4}$, much smaller than those typically considered in studies based on one-dimensional Bose-Hubbard Hamiltonians[22–24].

In passing we note that because of this large OS-repulsion the hydrogen atoms behave effectively as fermions, i.e., we obtain practically identical results independent of whether we treat the hydrogen atoms as fermions or as bosons. This can for example be understood by considering the fact that in the limit of $U \to \infty$ corresponding to hard-core bosons the Bose-Hubbard Hamiltonian Eq. (1) becomes equivalent to the spin-$\frac{1}{2}$ XXZ chain[47] so that some of the results for this model[48,49] can be transfered to the system considered in this study. Still it is important to realize that there are qualitative differences between considering hard-core bosons and having a large but finite U since in the latter case the double occupancy of one site is still possible.

Experimentally, at half coverage an ordered phase of adsorbed hydrogen at low temperatures has been observed[20,21]. To model this coverage, we considered a chain of length $L = 8$ filled with $N = 4$ hydrogen atoms. In order to characterize the specific phases we focus on renormalized local densities

$$\rho_i^0 \equiv \frac{\rho_i}{N/L} \,. \tag{10}$$

These renormalized local densities are plotted as a function of the tunneling parameter T and the NN-repulsion V in Fig. 2 for the first three sites $i = 1, 2, 3$. For a charge density wave, we expect a varying local density whereas it should be constant for the suprafluid phase. Indeed we find a region where the renormalized local densities are not constant. Note, however, that in the considered parameter range the renormalized local densities only vary between 0.85 and 1.15, i.e., there is still a rather small corrugation amplitude. The phase boundary between the phases is indicated by the black line.

The non-uniform densities plotted in Fig. 2 are based on one of the two degenerate ground-state solutions which exist because of the translational invariance of the Hamiltonian. This means that there is a spontaneous symmetry breaking. While also an uniform solution as a superposition of the two degenerate states is possible, when we sample the system, the system is cast on one of the two non-uniform eigenstates.

Another way to look at the structure of the solutions

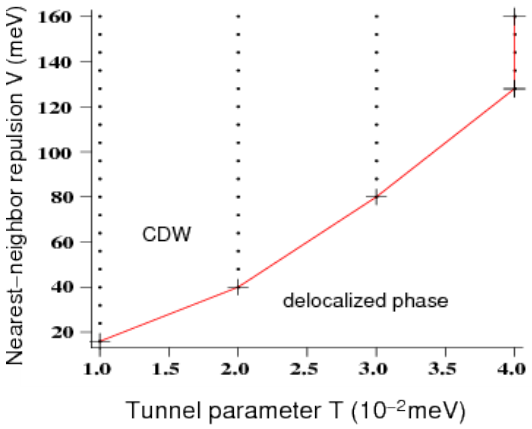

FIG. 4: Phase diagram for half filled chains as a function of the tunnel parameter T and the nearest-neighbor repulsion V with an on-site repulsion of $U = 1000$ meV. The small dots denote systems in which a CDW phase has been found.

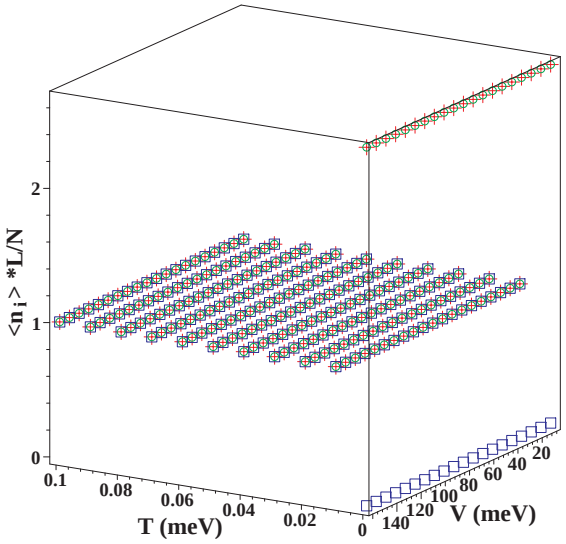

FIG. 5: Renormalized local densities $\rho_1 \equiv$ crosses, $\rho_2 \equiv$ squares and $\rho_3 \equiv$ circles over T and V for $L = 8$, $N = 3$ and $U = 1000$ meV.

is to consider the normalized density-density correlation function

$$\chi_i = \frac{< n_1 n_i > - < n_1 > \cdot < n_i >}{\sqrt{< n_1 - < n_1 >>^2 < n_i - < n_i >>^2}} \,. \qquad (11)$$

It corresponds to the conditional probability to find a particle at site i if there is a particle a site 1. In Fig. 3, we have plotted this normalized density-density correlation function for $L = 8$, $N = 2, 3, 4$, $U = 1000$ meV, $T = 0.02$ meV and $V = 70$ meV. Because of symmetry reasons, the correlation functions are symmetric with respect to site 5. It is obvious that for $N = 4$, the occupation of even and odd sites is strictly anti-correlated without any change in the magnitude of the correlation indicating the ordered solution.

To discuss the quantum phase transitions, we have plotted the phase diagram in Fig. 4. For small $T \leq 0.04\,\text{meV}$ and V sufficiently large we find charge density waves corresponding to an ordered adsorbate structure with an unit cell length of 2 sites. It is obvious that T has to be rather small together with a sizable nearest-neighbor repulsion in order to allow the existence of a CDW. Otherwise one obtains an uniform density. Note that this CDW at half-filling has been found before[23], however, in an entirely different parameter regime ($U = 1$, $T = 0.1$ and $V = 0.4$ in dimensionless units). Obviously, the high value of the on-site repulsion U used in our application already leads to an effective delocalization of the particles. Then, only a rather small value of the tunnel parameter is needed to stabilize the delocalized suprafluid phase.

The renormalized local densities as a function of T and V for $L = 8$ and $N = 3$, i.e. for a filling of $\rho = 3/8$, are shown in Fig. 5. Only for vanishing T, a CDW results with the localized densities being either 0 or 1, while for any $T > 0$ the uniform SF phase is stable. In fact, we obtain the same results for all particle numbers $N \neq 4$. This means that obviously only for half-filling a localized phase is possible. For all other fillings or coverages, a delocalized uniform phase is formed when the atoms are allowed to hop or tunnel ($T > 0$). These findings seem to be consistent with the experimental observation[20,21] of the existence of a localized hydrogen phase only in a sharp coverage window around half coverage.

With respect to the delocalized phase at lower coverages we note that it is constructed from the translationally symmetric superposition of states as described in eq. (6) resulting in a uniform density. Still, in each of the single states the distance between the particles is maximized, but this is only relevant for conditional distributions or pair correlation functions describing, e.g., the probability of finding a particle given that another particle is already located at a specific site. This is reflected in the density-density correlation functions χ_i plotted in Fig. 3 for $N = 2, 3$. The result for $N = 2$ is equivalent to the one obtained by Kühner *et al.*[23] for a filling of $\rho = 1/4$.

In order to study the influence of lattice imperfections on the resulting hydrogen phases, we introduced a lattice defect into our model by adding the term

$$H_{val} \equiv -\varepsilon \cdot \hat{n}_1 \qquad (12)$$

to the Hamiltonian (1). We considered a very weak perturbation making the site 1 energetically more favorable by $\varepsilon = 0.0005$ meV. The resulting renormalized local densities as a function of V and T for a filling of $\rho = 3/8$ are plotted in Fig. 6. With the defect we now find non-uniform local densities for small T. For larger T, however, the density becomes constant which means that for mobile particles the effect of the defect is washed out.

In order to see the detailed influence of the defect on the distribution of the particles, we plot in Fig. 7 the cor-

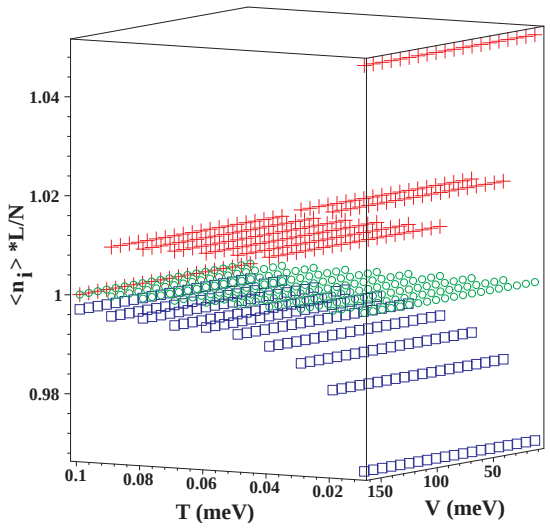

FIG. 6: Renormalized local densities $\rho_1 \equiv$ crosses, $\rho_2 \equiv$ squares and $\rho_3 \equiv$ circles as a function of the tunnel parameter T and the nearest-neighbor repulsion V for $L = 8$ and $N = 3$ with a perturbation $\varepsilon = 0.0005$ meV at site 1.

responding local densities $\rho_i, i = 1, ..., 8$ without renormalization for coverages $\rho = 1/4$ and $3/8$ for one particular set of parameters ($T = 0.02$ meV, $V = 70$ meV, $U = 1000$ meV) for which for half coverage a CDW occurs (see Fig. 4). Note that because of the periodic boundary conditions with chain length $L = 8$ the local densities have to be symmetric with respect to site 1 and also site 5. Since site 1 has been made energetically slightly more favorable, the densities show a maximum at this particular site. However, for both coverages there is only a small corrugation in the local densities which is a little bit larger for the higher coverage, though. This can be explained by the fact that because of the nearest-neighbor repulsion a higher coverage leads to a larger degree of localization. This was already observed on the one-particle level as a decrease in the vibronic band width with increasing coverage[13].

So far, we have not considered any coverages larger than 1/2. In fact, there is no need to do so because for our particular setup there is effectively a particle-hole-symmetry. As already mentioned, because of the high value $U = 1000$ meV for the on-site repulsion, a double occupancy of the adsorption sites is very unlikely. Consequently, there is a close relation between bosonic spin- and chargeless atoms and holes or vacancies on the chain. However, there are still small deviations from a perfect particle-hole symmetry are due to the large, but finite value of U.

In order to show this explicitly, we considered chains ($L = 8$) with coverages 3/8 and 5/8. For the less than half-filled chain we again introduced the perturbation eq. (13) with $\varepsilon = 0.0005$ meV. For the more than half-filled chain we introduced the defect with $\varepsilon = -0.0005$ meV. This means that we made site i slightly less favorable for atoms which also means that site i is

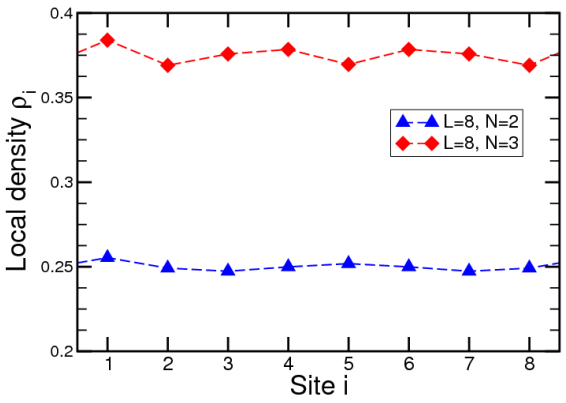

FIG. 7: Local densities ρ_i, $i = 1, ..., 8$, of a chain of length $L = 8$ occupied by $N = 2$ and $N = 3$ particles ($T = 0.02$ meV, $V = 70$ meV, $U = 1000$ meV) with a perturbation $\varepsilon = 0.0005$ meV at site 1.

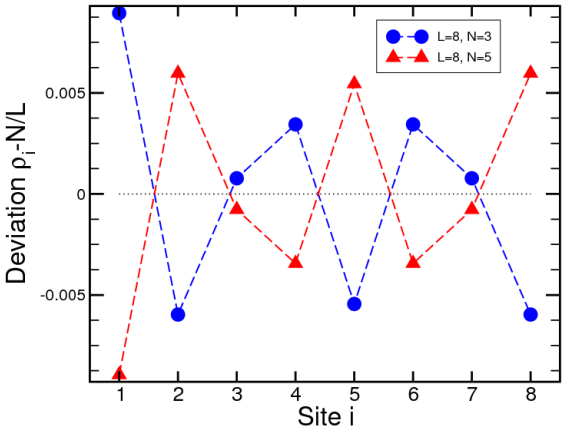

FIG. 8: Deviation δ_i of a chain of length $L = 8$ with particle densities $\rho = 3/8$ and $5/8$ and perturbations according to eq. (12) with $\varepsilon = 0.0005$ meV and $\varepsilon = -0.0005$ meV, respectively. The remaining parameters are $U = 1000$ meV, $T = 0.02$ meV, and $V = 70$ meV.

slightly more favorable for holes.

In Fig. 8, the deviation

$$\delta_i \equiv \rho_i - \frac{N}{L} \tag{13}$$

from the mean density is plotted in both cases. In fact, there is almost a perfect mirror symmetry in the deviations demonstrating that hydrogen atoms and vacancies are analogously distributed.

VI. LONG FINITE CHAINS

With respect to the findings of the last section, there still remains the question whether some of the results are artefacts of the periodic boundary conditions with a rather small unit cell. However, as mentioned above, the quickly growing dimension of the relevant Hilbert space prevents a direct diagonalization

for periodic systems with a larger unit cell. Therefore some approximate, but computationally less demanding method is required. In recent years, the **D**ensity **M**atrix **R**enormalization **G**roup (DMRG) method[22,23,28–30] has become very popular for simulating ground state properties of one-dimensional quantum systems. Since this method has hardly been used for surface science problems yet, we will briefly recall its basics and then show applications of the treatment for longer chains with various hydrogen coverages.

The pioneering work with respect to the DMRG method was done by S.R. White[28,29]. As in other quantum renormalization algorithms, the basic idea of this method is to start with a small system and then enlarge this system iteratively to the desired size. In each step, the set of basis functions is kept small by restricting it to the "most relevant" states. Before deciding about what are the most relevant states, DMRG embeds the system into a thermodynamic bath called the environment. The system and the environment together form the so-called superblock. The actual decision about the importance of the states for the system is made after tracing out the environment. The remaining reduced density matrix describing the system is then diagonalized and the d_S most probable states are kept as the relevant basis.

From its construction, DMRG introduces two different kinds of numerical errors. First, there is the natural truncation error which arises from the reduced basis transformations in each renormalization step. This error can be reduced by increasing d_S. The second error cannot be described in a clear mathematical way. In the corresponding literature[30], it is often refered to as the error through incorrectly "simulating the final system size". It has its origin in the fact that through the enlargement steps of the system wrong particle densities are realized on the chain since one is not able to add fractional bosons. To overcome this problem, one applies an additional algorithm after the system has grown to any desired size. This extra procedure is called the *finite length algorithm*. The idea is to take the chain of the desired length and to apply the steps of the infinite-system DMRG, but to keep the super-block size constant by growing the size of one block at the expense of the other. One loop of the finite length algorithm is called a *sweep*.

We have implemented our own version of the DMRG algorithm which follows in large parts the description in Ref. 30. However, there is one important difference to former DMRG applications. Since the on-site repulsion U is much larger than the other energy parameters, it has a decisive influence on the particle distribution. The states with more than one particle at a particular site that are in principle accessible are in practice impossible to realize. The contribution of these states to the ground state is therefore negligible. Since these states represent in fact the majority, it is sufficient within the DMRG algorithm to renormalize the system to a surprisingly small Hilbert space. Technically, this gave us the possibility to carry out a full diagonalization of the superblocks.

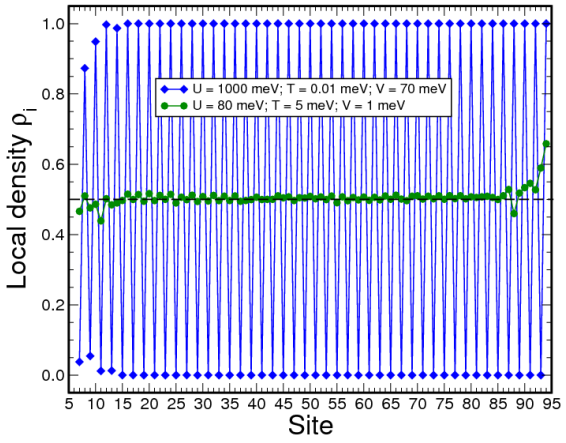

FIG. 9: Local densities ρ_i of a chain with length $L = 100$ and a coverage of $\rho = \frac{1}{2}$ obtained from DMRG calculations for two different sets of parameter given in the legend. 15 states and 3 sweeps were used.

In order to validate our implementation, we compared its results with those obtained with the open source package ALPS[50]. Running ALPS with $d_S = 128$ kept states and 4 finite length sweeps yielded ground state energies that differed only by less than 2 % from the results obtained with our implementation with 15 states and 3 sweeps.

As far as the boundaries of the chains are concerned, it would be desirable to use periodic boundary conditions. Unfortunately, the DMRG results are much less reliable for periodic boundary conditions[30]. Therefore we have chosen open boundary conditions. One has to be aware that this also means that boundary effects are introduced which have been observed before to be quite significant[23] and which also influence the results in the parameter regime considered by us, as will become obvious in the following.

First we focus on half-filled chains where we expect the formation of a CDW. Tests showed that a chain length of $L = 100$ is sufficient, for longer chains no qualitative changes occur, as was also found in a previous study[23]. In Fig. 9, the local densities for $U = 1000$ meV, $T = 0.01$ meV and $V = 70$ meV are plotted. Indeed we find an ordered localized structure. Note, however, that the amplitude of the local-density fluctuations is much larger compared to the calculations for $L = 8$ with periodic boundary conditions. While now the densities alternate practically between zero and one, for periodic boundary conditions the deviation from the mean value 0.5 is below 10 % in this parameter regime (see Fig. 2).

This is obviously a boundary effect. At the edge sites, the nearest-neighbor repulsion is only active from one side. This leads to a high probability for the occupation of the edge sites by the hydrogen atoms which induces the large amplitude local-density fluctuations. There is another consequence of this preferential occupation of the edge site. From either site of the chain a CDW builds up.

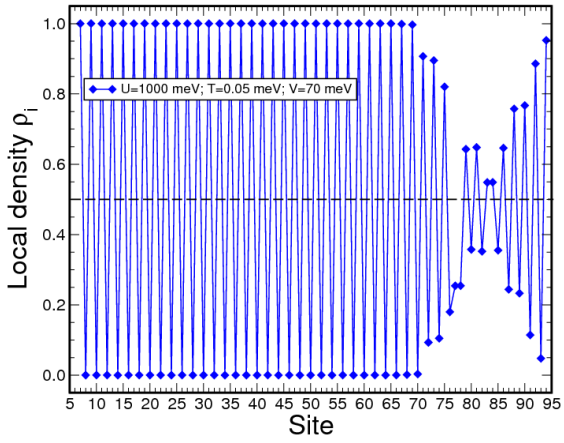

FIG. 10: Local densities ρ_i of a chain with length $L = 100$ and a coverage of $\rho = \frac{1}{2}$ obtained from DMRG calculations for $U = 1000$ meV, $T = 0.05$ meV and $V = 70$ meV. Between sites 65 and 92, an anti-phase boundary occurs.

However, since we have an even number of sites in order to realize a coverage of $\rho = 1/2$, these two CDWs are phase-shifted by π. Consequently, an anti-phase boundary has to occur where these two CDWs meet. In Fig. 9 it is not visible since it occurs at the very left edge. Interestingly enough, the anti-phase boundary moves towards the middle of the chain when the tunnel parameter is increased. For $T = 0.05$ meV, there is an extended region of the anti-phase boundary between sites 65 and 92, as Fig. 10 demonstrates. Using the ALPS code, such anti-phase boundaries were obtained as well. Note that with periodic boundary conditions, we did not obtain a CDW for such a larger value of T (see Fig. 4) indicating that the boundary effects extend the stability range of the localized CDW phase.

In Fig. 9, results for the parameters used by Astaldi *et al.* ($U = 80$ meV, $V = 1$ meV, $T = 5$ meV)[13] are also included. For such a small on-site repulsion and a large T/V ratio, a delocalized SF phase results. It is important to realize that the parameters chosen by Astaldi *et al.* were meant to describe a hydrogen atom in a higher vibrationally excited state in which the dispersion of the corresponding vibronic band and consequently also the relevant tunnel parameter T is much larger[11,40] so that it is not surprising that a delocalized phase results.

In the next step, the particle density is lowered to $\rho = 1/3$. In order to simulate this density within the DMRG formalism on a finite chain, the chain length is set to $L = 102$. According to Fig. 11, for an on-site repulsion of $U = 1000$ meV and small tunnel parameters T we now obtain a CDW with periodicity 3, in contrast to the chain with periodic boundary conditions where no CDW at such a coverage was observed. However, the fluctuations around the mean value $\rho = 1/3$ are smaller than for $\rho = 1/2$. Interestingly enough, when the tunnel parameter is increased from $T = 0.01$ meV to $T = 0.05$ meV, the amplitude of the density oscillations is even increased.

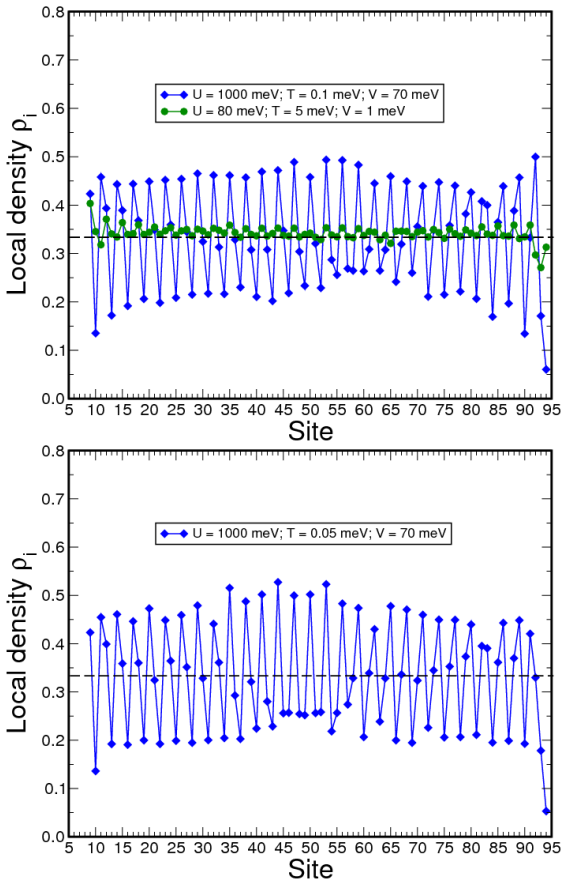

FIG. 11: Local densities ρ_i of a chain with length $L = 102$ and a coverage of $\rho = \frac{1}{3}$ obtained from DMRG calculations for two different sets of parameter given in the legend.

For the conditions considered by Astaldi *et al.*[13], the local densities become more uniform again. Still, there is some oscillatory structure left with amplitudes that are larger than for a coverage of $\rho = 1/2$. Note that also for the system considered by Kühner *et al.*[23] ($U = 1$, $T = 0.1$ and $V = 0.4$ in dimensionless units) a CDW has only been found for half-filling, but not for other fillings.

Finally, we have considered a coverage of $\rho = 1/4$ on a finite chain with length $L = 120$ (Fig. 12). Again we obtain a localized CDW phase, here with periodicity 4, again in contrast to the situation with periodic boundary conditions. This shows that strong perturbations or defects can induce an ordered structure that would not be stable in a perfectly translationally invariant system. Still, the amplitude of the oscillations for $U = 1000$ meV is further reduced. As already discussed in the context of Fig. 7, the effect of the nearest-neighbor repulsion that leads to a higher degree of localization for the larger coverages is reduced at lower coverages.

Furthermore, as in Fig. 11 for a coverage of $\rho = 1/3$ we observe first a stabilization of the ordered structure with increasing tunnel parameter T and then a reduction of the oscillations towards a delocalized SF-Phase for a higher T/V ratio. Obviously, a larger tunnel parameter T

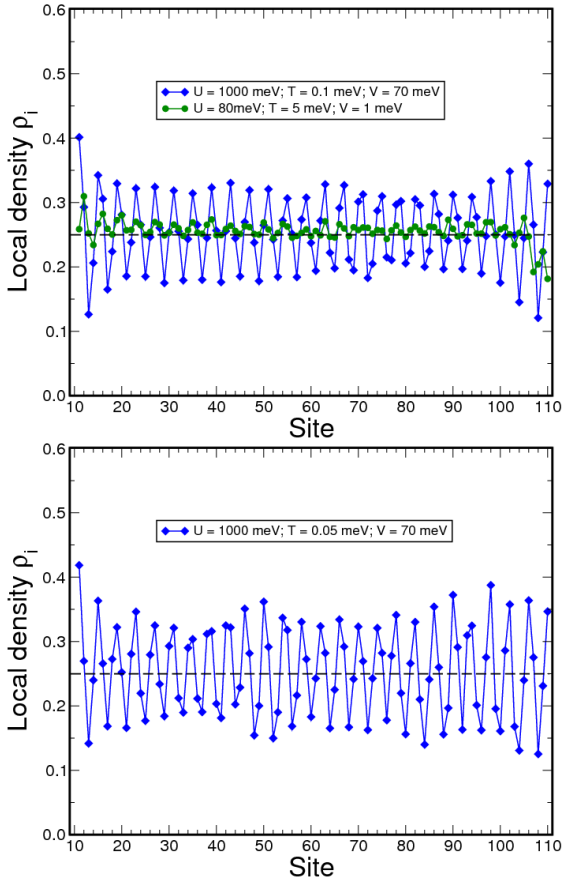

FIG. 12: Local densities ρ_i of a chain with length $L = 120$ and a coverage of $\rho = \frac{1}{4}$ obtained from DMRG calculations for two different sets of parameter given in the legend.

first increases the influence of the nearest-neighbor repulsion before it leads to a delocalization. But again, for the conditions of vibrationally excited hydrogen atoms considered by Astaldi *et al.*[13], the remaining amplitude of the oscillations is even larger than for coverage $\rho = 1/3$. Apparently, the effect of increasing the T/V ratio is less strong for smaller coverages.

This strong influence of boundary effects on the resulting phase also means that one has to be cautious in this particular parameter regime in applying results for finite chains, as obtained in DMRG calculations, to infinite periodic chains.

VII. CONCLUDING REMARKS

Employing a Bose-Hubbard Hamiltonian, we have addressed the quantum delocalization and quantum phase transitions of hydrogen atoms adsorbed in one-dimensional chains on metal surfaces. These systems are characterized by a large on-site repulsion U, a very small overlap or tunnel parameter T and a sizable nearest-neighbor repulsion V. Using periodic boundary conditions and a direct diagonalization scheme, we find, as other groups before, that an ordered localized structure can only be obtained for a coverage of $\rho = 1/2$ which is consistent with experimental observations of hydrogen adsorption phases at low temperatures. Apparently, for $\rho < 1$, $\rho \neq 1/2$, quantum particles are always uniformly delocalized in a periodic translationally invariant chain if there is a non-vanishing overlap between adjacent sites ($T > 0$).

For the particular systems considered in this study, some properties result that were not found in one-dimensional bosonic systems with generic parameters studied before. First of all, the large on-site repulsion makes a double occupancy of the adsorption sites energetically very costly having an effective particle-hole symmetry as a consequence. Second, there is a rather strong influence of perturbations or defects on the resulting quantum phases. If the perturbations are sufficiently strong, they can induce ordered structures at other coverages than $\rho = 1/2$ in an extended region. This also means that in this parameter regime the results for finite chains can not be applied to infinite systems without caution.

Acknowledgment

We thank Christian Carbogno and Christian Mosch for their technical support in the programming work.

* New Address: Forschungszentrum Jülich, D-52425 Jülich, Germany

[1] I. Bloch, J. Dalibard, and W. Zwerger, Rev. Mod. Phys. **80**, 885 (2008).
[2] M. Greiner, O. Mandel, T. Esslinger, T. W. Hänsch, and I. Bloch, Nature **415**, 39 (2002).
[3] G. Ertl, Angew. Chem. Int. Ed. **47**, 3524 (2008).
[4] K. Christmann, Surf. Sci. Rep. **9**, 1 (1988).
[5] M. Nishijima, H. Okuyama, N. Takagi, T. Aruga, and W. Brenig, Surf. Sci. Rep. **57**, 113 (2005).
[6] S. Sakong and A. Groß, Surf. Sci. **525**, 107 (2003).
[7] J. Greeley and M. Mavrikakis, J. Phys. Chem. B **109**, 3460 (2005).
[8] M. J. Puska et al., Phys. Rev. Lett. **51**, 1081 (1983).
[9] M. J. Puska and R. M. Nieminen, Surf. Sci. **157**, 413 (1985).
[10] L. J. Lauhon and W. Ho, Phys. Rev. Lett. **85**, 4566 (2000).
[11] W. Z. Lai, D. Q. Xie, J. L. Yang, and D. H. Zhang, J. Chem. Phys. **121**, 7434 (2004).
[12] S. C. Badescu et al., Phys. Rev. Lett. **88**, 136101 (2002).
[13] C. Astaldi, A. Bianco, S. Modesti, and E. Tosatti, Phys. Rev. Lett. **68**, 90 (1992).
[14] C. T. Rettner and D. J. Auerbach, Phys. Rev. Lett. **77**, 404 (1996).

[15] A. Groß and M. Scheffler, Phys. Rev. Lett. **77**, 405 (1996).
[16] C. T. Rettner and D. J. Auerbach, Chem. Phys. Lett. **253**, 236 (1996).
[17] A. Groß and M. Scheffler, Phys. Rev. B **57**, 2493 (1998).
[18] A. Groß, J. Chem. Phys. **110**, 8696 (1999).
[19] N. Takagi et al., Phys. Rev. B **53**, 13767 (1996).
[20] A. T. Hanbicki, P. J. Rous, and E. W. Plummer, Phys. Rev. B **67**, 205405 (2003).
[21] D. Farías, M. Patting, and K. H. Rieder, J. Chem. Phys. **117**, 1797 (2002).
[22] T. D. Kühner and H. Monien, Phys. Rev. B **58**, R14741 (1998).
[23] T. D. Kühner, S. R. White, and H. Monien, Phys. Rev. B **61**, 12474 (2000).
[24] G. G. Batrouni, F. Hébert, and R. T. Scalettar, Phys. Rev. Lett. **97**, 087209 (2006).
[25] M. P. A. Fisher, P. B. Weichman, G. Grinstein, and D. S. Fisher, Phys. Rev. B **40**, 546 (1989).
[26] P. Niyaz, R. T. Scalettar, C. Y. Fong, and G. G. Batrouni, Phys. Rev. B **44**, 7143 (1991).
[27] A. Groß, Surf. Sci. **500**, 347 (2002).
[28] S. R. White, Phys. Rev. Lett. **69**, 2863 (1992).
[29] S. R. White, Phys. Rev. B **48**, 10345 (1993).
[30] U. Schollwöck, Rev. Mod. Phys. **77**, 259 (2005).
[31] J. Hubbard, Proc. Roy. Soc. A **276**, 238 (1963).
[32] E. Dagotto, Rev. Mod. Phys. **66**, 763 (1994).
[33] D. Jaksch, C. Bruder, J. I. Cirac, C. W. Gardiner, and P. Zoller, Phys. Rev. Lett. **81**, 3108 (1998).
[34] S. Wilke, D. Hennig, R. Löber, M. Methfessel, and M. Scheffler, Surf. Sci. **307**, 76 (1994).
[35] R. Löber and D. Hennig, Phys. Rev. B **55**, 4761 (1997).
[36] V. Ledentu, W. Dong, P. Sautet, G. Kresse, and J. Hafner, Phys. Rev. B **57**, 12482 (1998).
[37] M. Lischka and A. Groß, Phys. Rev. B **65**, 075420 (2002).
[38] A. Roudgar and A. Groß, J. Electroanal. Chem. **548**, 121 (2003).
[39] A. Groß, *Theoretical surface science – A microscopic perspective*, Springer, Berlin, 2nd edition, 2009.
[40] T. R. Mattsson, G. Wahnström, L. Bengtsson, and B. Hammer, Phys. Rev. B **56**, 2258 (1997).
[41] V. Pouthier and J. C. Light, J. Chem. Phys. **113**, 1204 (2000).
[42] W. Lai and D. Xie, Surf. Sci. **550**, 14 (2004).
[43] A. Groß and A. Dianat, Phys. Rev. Lett. **98**, 206107 (2007).
[44] A. Groß, ChemPhysChem **11**, 1374 (2010).
[45] G. Kresse and J. Furthmüller, Phys. Rev. B **54**, 11169 (1996).
[46] J. P. Perdew, K. Burke, and M. Ernzerhof, Phys. Rev. Lett. **77**, 3865 (1996).
[47] T. Matsubara and H. Matsuda, Prog. Theor. Phys. **16**, 569 (1956).
[48] H.-J. Mikeska and A. K. Kolezhuk, One-dimensional magnetism, in *Quantum Magnetism*, edited by U. Schollwöck, J. Richter, D. Farnell, and R. Bishop, volume 645 of *Lecture Notes in Physics*, pages 1–83, Springer, Berlin, 2004.
[49] D. Gobert, C. Kollath, U. Schollwöck, and G. Schütz, Phys. Rev. E **71**, 036102 (2005).
[50] A. Albuquerque et al., J. Magn. Magn. Mater. **310**, 1187 (2007).